

# Real-Time Detection of Rectilinear Sources for Wireless Communication Signals

Sithan Kanna, Min Xiang, Danilo P. Mandic

Department of Electrical and Electronic Engineering

Imperial College London, London SW7 2AZ, United Kingdom.

Email: {ssk08, m.xiang13, d.mandic}@ic.ac.uk

**Abstract**—This paper proposes a real-time detector of rectilinearity of signals received by an antenna array. A rectilinear source is characterised by having a circularity coefficient of unity and it represents a real-valued source with an arbitrary phase shift. Real-time detection of rectilinearity has been introduced as a new challenge in communications since identifying the rectilinearity of the sources would help designers choose between strictly linear and widely linear beamformers. The proposed real-time detector of rectilinearity, first separates the sources with an online blind source separation (BSS) algorithm, then estimates the circularity coefficient of the separated sources using a real-time circularity tracker. We exploit the result that the variance of the circularity tracker is null for rectilinear signals to tune the algorithm for rapid convergence and robust detection. Simulations on synthetic communication data support the analysis and claims.

**Index Terms**—Rectilinearity, CLMS, adaptive filters, blind source separation, circularity tracker.

## NOTATION

Lower-case letters are used to denote scalars, boldface letters for vectors and boldface upper-case letters for matrices. The symbol  $(\cdot)^*$  denotes complex conjugation, while  $(\cdot)^T$  and  $(\cdot)^H$  are used for transposition and conjugate transposition. The subscript  $k$  is used as a time index and  $\mathbf{E}\{\cdot\}$  represents the statistical expectation operator. The operator  $|z|$  is used to represent the magnitude of a complex variable  $z$ .

## I. INTRODUCTION

Adaptive beamforming is crucial for wireless communication networks as it is used to extract signals of interest (SOI) by rejecting the interference and noise for signals and channels with time varying statistics. Consider a uniform linear array (ULA) of  $N$  sensors which receives a signal of interest  $m_k$  at time instant  $k$  according to the following relationship

$$\mathbf{x}_k = m_k \mathbf{s} + \mathbf{n}_k \quad (1)$$

where  $\mathbf{x}_k \in \mathbb{C}^{N \times 1}$  is the measurement vector with the entries from each ULA sensor,  $\mathbf{s} \in \mathbb{C}^{N \times 1}$  is the steering or the channel vector of the SOI and  $\mathbf{n}_k \in \mathbb{C}^{N \times 1}$  is the total noise vector.

Traditional complex-valued adaptive beamformers were derived as generic extensions of their real-valued counterparts where the signal  $m_k$  is recovered by a strictly linear adaptive filter  $y_k = \mathbf{h}_k^H \mathbf{x}_k$  with output  $y_k$  which corresponds to the recovered signal and the input  $\mathbf{x}_k$  is from the antenna array

measurements given in (1). The beamforming filter weight vector  $\mathbf{h}_k$  is adaptively estimated by minimising the mean square error (MSE) cost function given by

$$\mathcal{J}_{\text{MSE}}(\mathbf{h}_k) = \mathbf{E} \left\{ |m_k - y_k|^2 \right\} = \mathbf{E} \left\{ |m_k - \mathbf{h}_k^H \mathbf{x}_k|^2 \right\}. \quad (2)$$

The strictly linear solution to the cost function in (2) is only optimal for a restricted class of signals which are second order circular and a widely linear beamformer is required for a general class of non-circular signals. The widely linear beamformer is able to recover non-circular SOI using a widely linear model which utilizes both  $\mathbf{x}_k$  and its conjugate  $\mathbf{x}_k^*$  to give  $y_k = \mathbf{h}_k^H \mathbf{x}_k + \mathbf{g}_k^H \mathbf{x}_k^*$ . The filter weight vectors  $\mathbf{h}_k$  and  $\mathbf{g}_k$  are also derived by minimising the MSE cost function given by [1]

$$\mathcal{J}_{\text{MSE}}(\mathbf{h}_k, \mathbf{g}_k) = \mathbf{E} \left\{ |m_k - \mathbf{h}_k^H \mathbf{x}_k - \mathbf{g}_k^H \mathbf{x}_k^*|^2 \right\}. \quad (3)$$

Adaptive (real-time) beamformers are derived by minimising the cost functions given in (2) and (3) either via the stochastic gradient descent to form the complex least mean square (CLMS) [2] and augmented CLMS (ACLMS) algorithms [3], [4] or by minimising sum of the error squares recursively to form the recursive least squares (RLS) [5] and widely linear RLS (WL-RLS) algorithms [6].

For an  $N$ -sensor antenna array, widely linear beamformers are able to process more than the conventional limit of  $N - 1$  sources when two or more of the sources are rectilinear [7]. A rectilinear source is a special case of a complex-valued source as it is effectively a single real-valued source with an arbitrary phase shift. However, since the widely linear solution for (3) requires twice the number of complex coefficients compared to the strictly linear solution for (2), this results in an increase in computational complexity. Moreover, doubling the number of coefficients for adaptive filters results in a larger steady state excess MSE [8]. Therefore, it is important to determine the rectilinearity of the sources prior to employing either a strictly linear or a widely linear adaptive beamformer<sup>1</sup>.

The idea of detecting the rectilinearity of sources after a blind source separation (BSS) step for wireless communication signals was first suggested in [7], where the sample covariance and pseudocovariance were used to estimate the rectilinearity

<sup>1</sup>Note that we have assumed that the criterion for choosing between strictly linear and widely linear processing is solely based on the number of sources that can be separated.

of the signal. Other more sophisticated tools to estimate the non-circularity (hence, rectilinearity) of signals have been suggested in the past, see [9]–[11]. However, as most of these algorithms, including the approach in [7], are block-based, they are not suitable for real-time applications or for non-stationary data.

To this end, we show that the rectilinearity detection idea in [7] can be extended for online applications by a combination of an adaptive (online) BSS algorithm [12] and a real-time rectilinearity tracker based on the circularity tracker in [13].

## II. BACKGROUND

### A. Online Circularity Tracker

The *circularity quotient* of a zero-mean random variable (r.v.)  $s_k \in \mathbb{C}$ , is given by [14]

$$\rho_s \stackrel{\text{def}}{=} \frac{p_s}{c_s} \quad (4)$$

where  $c_s = \mathbb{E}\{|s_k|^2\}$  and  $p_s = \mathbb{E}\{s_k^2\}$  are respectively the covariance and pseudocovariance of the signal  $s_k$ . The *circularity coefficient* of the signal  $s_k$  is given by the magnitude of the circularity quotient i.e.  $|\rho_s|$ . A signal is considered to be rectilinear if its circularity quotient can be expressed as  $\rho_s = e^{j\phi}$ , with an arbitrary phase shift  $\phi$ . Therefore, rectilinear signals have circularity coefficients  $|\rho_s| = 1$ .

To understand the principle of the online circularity (and rectilinearity) tracker, first consider the problem of using  $s_k$  to estimate its complex conjugate,  $s_k^*$ , linearly using a coefficient  $w$  as

$$\hat{s}_k^* = w^* s_k \quad (5)$$

where  $\hat{s}_k^*$  denotes the estimate of the complex conjugate of  $s_k$ . Since it is impossible to find a single coefficient  $w$  for all realisations of  $s_k$ , we opt to employ a minimum mean square error (MMSE) estimation, whereby the optimal value of  $w$  is found by minimising the cost function

$$\mathcal{J}_{\text{MSE}}(w) = \mathbb{E}\{|s_k^* - w^* s_k|^2\} \quad (6)$$

The optimal value of  $w$ , denoted by  $w_{\text{opt}}$ , that minimizes the cost function in (6) is then given by the Wiener solution

$$w_{\text{opt}} = \frac{\mathbb{E}\{s_k^2\}}{\mathbb{E}\{|s_k|^2\}} = \rho_s \quad (7)$$

From (7), we can see that the circularity quotient can be interpreted as the strictly linear MMSE solution for estimating the complex conjugate of a random variable from the original random variable itself. Using the interpretation in (7), we are able to derive an adaptive estimator of the circularity quotient using the CLMS, given by [13]

$$\hat{s}_k^* = \hat{\rho}_k^* s_k \quad (8a)$$

$$\hat{\rho}_{k+1} = \hat{\rho}_k + \mu (s_k^* - \hat{s}_k^*)^* s_k \quad (8b)$$

where the parameter  $\mu$  in (8b) is the step-size which determines the trade-off between the convergence rate and the

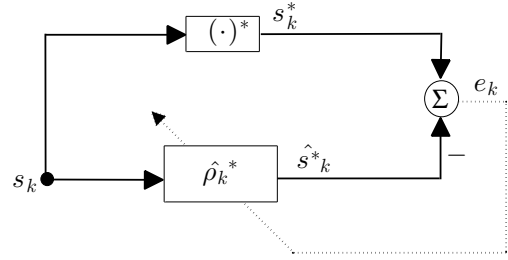


Fig. 1. Block diagram of the circularity (or rectilinearity) tracker.

steady-state error of the algorithm [2].

### Statistical properties of the real-time circularity tracker.

From [13], we observe that the statistical properties (mean and variance) of the circularity coefficient estimate  $\hat{\rho}_k$  is identical to the CLMS algorithm. Namely, the online circularity tracker is asymptotically unbiased

$$\lim_{k \rightarrow \infty} \mathbb{E}\{\rho_s - \hat{\rho}_k\} = 0 \iff 0 < \mu < 2/c_s \quad (9)$$

where  $c_s$  is the covariance (power) of the input signal  $s_k$ . Secondly, the steady-state covariance of the estimation error  $\rho_s - \hat{\rho}_k$  (misadjustment) is

$$\lim_{k \rightarrow \infty} \mathbb{E}\{|\rho_s - \hat{\rho}_k|^2\} = \mu c_s \frac{(1 - |\rho_s|^2)(2 - |\rho_s|^2)}{2 - \mu c_s(2 + |\rho_s|^2)} \quad (10)$$

**Remark #1:** The weight error covariance (misadjustment) depends on the degree of impropriety of the signal and is lower for signals that are less proper. Moreover, the steady state covariance for the circularity estimate is null for rectilinear signals which have a circularity coefficient of  $|\rho_s| = 1$ .

### B. Online Blind Source Separation

Consider representing the signal in (1) as a mixture of  $M$  sources corrupted by background noise  $\mathbf{n}_{b,k}$ , such that

$$\mathbf{x}_k = \sum_{\ell=1}^M s_{\ell,k} \mathbf{a}_\ell + \mathbf{n}_{b,k} = \mathbf{A} \mathbf{s}_k + \mathbf{n}_{b,k} \quad (11)$$

where  $\mathbf{s}_k = [s_{1,k}, s_{2,k}, \dots, s_{M,k}]^T$  is a vector containing all the sources  $s_{\ell,k}$ , the columns of  $\mathbf{A}$  are the channel vectors  $\mathbf{a}_\ell$  of the sources  $\ell = \{1, \dots, M\}$ , and  $\mathbf{n}_{b,k}$  is the background noise assumed to be zero-mean, circular and Gaussian. At each time instant  $k$ , the separation task can be expressed as

$$\mathbf{y}_k = \mathbf{B}_k \mathbf{x}_k \quad (12)$$

where  $\mathbf{x}_k$  is the mixture of sources given in (11).

In this work, we employ the well known class of equivariant adaptive separation via independence (EASI) algorithms for adaptive (real-time) separation of instantaneous mixtures of blind sources [12], [15]. A serial update of the de-mixing matrix  $\mathbf{B}_k$  in the EASI algorithm is derived using the relative gradient of the objective function. Considering the presence of non-circular sources, we also modify the normalised version of the EASI algorithm in [12] using the concept of removing

the unitary constraint on the de-mixing matrix as suggested by [16] to give the de-mixing matrix update as

$$\mathbf{B}_{k+1} = \mathbf{B}_k + \lambda \frac{\mathbf{I} - \mathbf{g}(\mathbf{y}_k) \mathbf{y}_k^H}{1 + \lambda |\mathbf{y}_k^H \mathbf{g}(\mathbf{y}_k)|} \mathbf{B}_k \quad (13)$$

where  $\lambda$  is a positive step-size which governs the trade-off between convergence rate and separation accuracy.

The function  $\mathbf{g}(\mathbf{y}) = [g_1(y_1), g_2(y_2), \dots, g_N(y_N)]^T$  is a component-wise nonlinear function of the elements in  $\mathbf{y} = [y_1, y_2, \dots, y_N]^T$ . Choosing the optimal nonlinear function  $\mathbf{g}(\cdot)$  is difficult in practice since it depends on the statistical distributions of the sources which are unknown *a priori*. Having said that, a simple nonlinear function for non-Gaussian sources is  $g_i(y_i) = y_i f_i(|y_i|^2) \forall i \in \{1, 2, \dots, N\}$  where  $f_i(\cdot)$  is any real-valued function that exploits higher order information of the data [17]. The simplest choice of  $f_i$  is  $f_i(|y_i|^2) = |y_i|^2$  which gives [18], [19]

$$g_i(y_i) = y_i |y_i|^2. \quad (14)$$

### III. PROPOSED ALGORITHM: REAL-TIME DETECTION OF RECTILINEAR SOURCES

Consider the problem of estimating the rectilinearity of the sources within the noisy instantaneous mixture  $\mathbf{x}_k$  given in (11) at each time instant  $k$ . As a new measurement  $\mathbf{x}_k$  arrives, the proposed algorithm separates the sources, updates the de-mixing matrix  $\mathbf{B}_k$  and updates the circularity coefficient of the separated sources.

Specifically, at each time instant  $k$ , the following steps are repeated:

- for**  $\hat{M} = \{1, 2, 3, \dots, N\}$  **do**
- 1) Separate the  $\hat{M}$  blind sources which are assumed to be mixed in  $\mathbf{x}_k$  using (12) and update the de-mixing matrix  $\mathbf{B}_k$  using (13).
  - 2) Update the circularity quotient  $\rho_{y_i,k}$  for each element of  $\mathbf{y}_k = [y_{1,k} \dots, y_{\hat{M},k}]^T$  using (8a) – (8b).
  - 3) If the circularity coefficient  $|\rho_{y_i,k}| > \beta_{\hat{M}}$ , then source  $y_i$  is rectilinear.

**end for**

Since the number of sources  $M$  is unknown *a priori*, we separate the sources for each  $\hat{M} = \{1, 2, 3, \dots, N\}$ .

**Remark #2:** Although rectilinear sources have a circularity coefficient of unity, the separated sources would be corrupted by noise which may not be rectilinear. Therefore, even in the case of perfect separation, the separated source which is fed into the rectilinear tracker will never be perfectly rectilinear. Consequently, the detection threshold is chosen to be  $\beta_{\hat{M}} < 1$ .

The optimal choice of the detection threshold  $\beta_{\hat{M}}$  is out of the scope of this paper and in our simulations we used a value that was close to one, e.g.  $\beta_{\hat{M}} = 0.9$ .

## IV. SIMULATIONS

### A. Case Study #1: Real-Time Detection of Rectilinearity

We considered a ULA of 4 omnidirectional sensors, equispaced half a wave length apart, that received four statistically independent narrow band sources which were either binary phase shift keying (BPSK) or quadrature phase shift keying (QPSK) sources that were corrupted by zero-mean white Gaussian noise. The directions of arrival of the sources were  $\{-45^\circ, 8^\circ, -13^\circ, 30^\circ\}$  and the SNR was chosen to be 10 dB.

The type of narrowband signals received by the antenna array changes so that for the first 500 samples, the sources were chosen to be four independent QPSK signals (circular, non-rectilinear) and for the last 500 samples, three independent BPSK signals (rectilinear) and one independent QPSK signal were chosen. The modified EASI shown in (13) was applied to separate sources hidden in the observed signal. The separation matrix  $\mathbf{B}_k$  was initialised with random entries and the nonlinear function  $\mathbf{g}(\cdot)$  given in (14) was used.

For the first 100 iterations, the step-size  $\lambda$  was set to be relatively large ( $\lambda = 0.1$ ) for rapid convergence. Then value of  $\lambda$  was reduced to  $\lambda = 0.01$  for steady-state accuracy. Figure 2 and Figure 3 show the constellations of separated sources ( $\hat{M} = 4$ ) within the first 500 samples and the last 500 samples respectively. The separated sources in Figure 2 appear noisier than the sources in Figure 3 since a larger step-size  $\lambda$  was used for the first 100 samples.

For the circularity tracker, the initial estimates were set to be zero while the step-size was chosen to be relatively large,  $\mu = 0.2$ , for a fast convergence rate. The evolution of the circularity coefficient estimates of the sources is shown in Figure 4. The estimates of the circularity coefficients of the four separated QPSK sources oscillate between 0 (the true value of the circularity coefficient) and 0.5. This large fluctuation is attributed to the background noise and the relatively large step-size  $\mu$  which was chosen so that the algorithm converges rapidly. Nevertheless, from samples 500 onwards, the circularity coefficient estimates of the three separated BPSK sources converge to a value close to 1. As mentioned in Remark #2, this is due to the fact that the sources are corrupted by non-rectilinear noise. When the estimated number of sources was not equal to the true number ( $\hat{M} = 1, 2, 3$ ), the circularity coefficients were all less than the threshold  $\beta_{\hat{M}} = 0.9$ .

### B. Case Study #2: Steady-State Misadjustment of the Circularity Tracker

Next, we tested the steady-state misadjustment of the circularity tracker for various levels of non-circularity. We generated a 1000-sample long white Gaussian noise with unit covariance  $c = 1$  and varying degrees of pseudocovariance  $p$  (hence circularity coefficients,  $|\rho|$ ) and applied the circularity tracker to estimate the circularity coefficient. The steady-state misadjustment was computed over 5000 independent

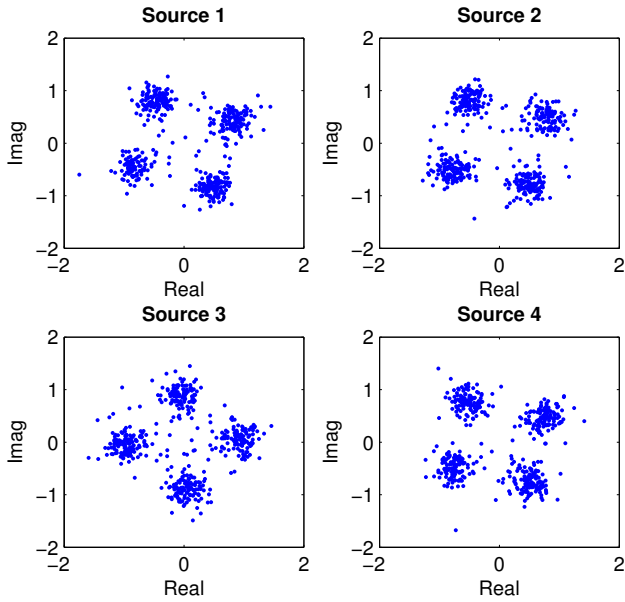


Fig. 2. Constellations of four separated QPSK sources (circular, non-rectilinear) present in the first 500 samples of the received signal.

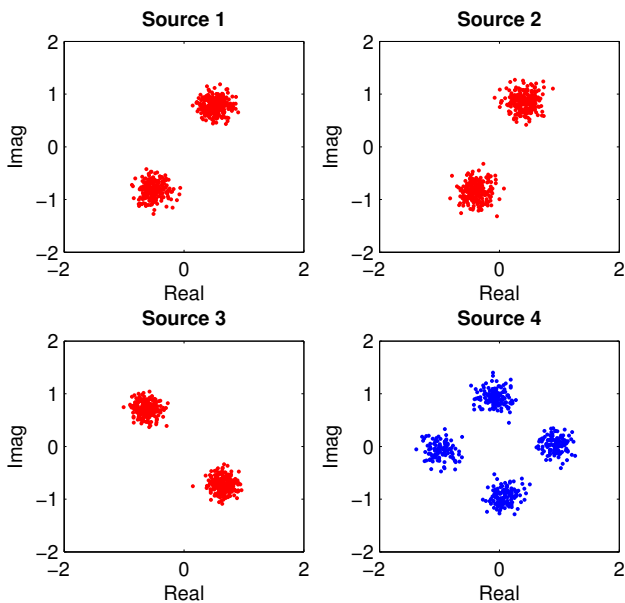


Fig. 3. Sources 1–3 show the constellations of three separated BPSK sources (rectilinear) while Source 4 shows the constellation of one separated QPSK source (circular, non-rectilinear) present in the second 500 samples of the received signal.

simulations using the formula

$$\mathcal{M} = \frac{1}{5000} \sum_{i=1}^{5000} \|\rho\| - |\hat{\rho}_{\infty}(i)|^2 \quad (15)$$

where  $|\rho|$  was the true circularity coefficient and  $|\hat{\rho}_{\infty}(i)|$  was the steady-state estimate of the circularity coefficient for simulation  $i$ . Figure 5 compares the theoretical steady-state

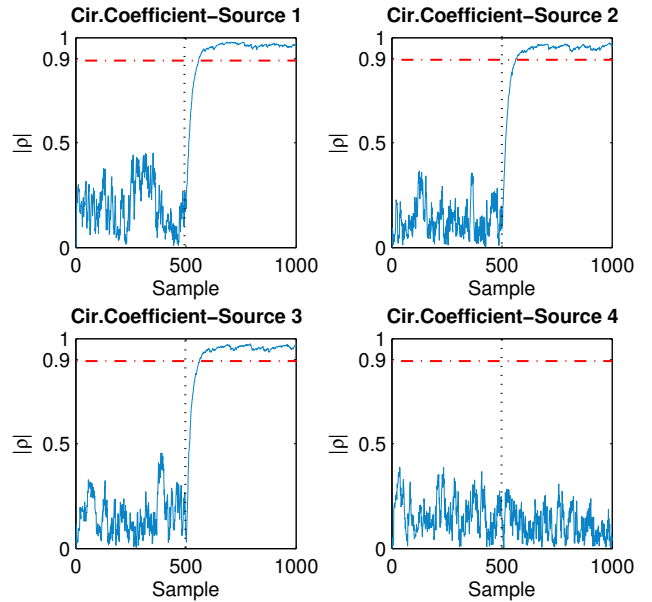


Fig. 4. Circularity coefficient estimates of the separated sources. Detection threshold was chosen to be  $\beta_{\hat{\mathcal{M}}} = 0.9$ .

misadjustment given in (10) to the empirical estimate from the Monte-Carlo simulations given in (15). Conforming with the analysis, the steady-state misadjustment of the circularity coefficient estimate decreases with increasing levels of non-circularity and reaches zero for rectilinear signals ( $|\rho| = 1$ ).

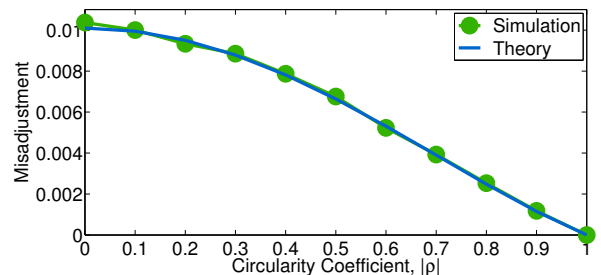


Fig. 5. Steady-state misadjustment of the circularity tracker for varying levels of signal non-circularity.

## V. CONCLUSION

We have proposed a novel real-time detector of rectilinearity for wireless communication signals. The proposed algorithm combines an online BSS algorithm to separate the signal received by an antenna array and a recently introduced circularity tracker to detect the rectilinearity of the separated sources. The fact that the circularity tracker has a steady-state misadjustment of null for rectilinear signals was exploited to tune the algorithm with a high detection threshold to increase robustness and a large step-size for rapid convergence. The proposed method was verified using synthetically generated BPSK and QPSK sources.

## REFERENCES

- [1] P. Chevalier, J.-P. Delmas, and A. Oukaci, "Optimal widely linear MVDR beamforming for noncircular signals," in *Proc. of the IEEE Intl. Conf. on Acoust. Speech and Signal Process. (ICASSP)*, April 2009, pp. 3573–3576.
- [2] B. Widrow, J. McCool, and M. Ball, "The complex LMS algorithm," *Proc. of the IEEE*, vol. 63, no. 4, pp. 719–720, 1975.
- [3] S. Javidi, M. Pedzisz, S. L. Goh, and D. P. Mandic, "The augmented complex least mean square algorithm with application to adaptive prediction problems," in *Proc. of the IAPR Workshop Cognitive Information Processing Syst.*, June 2008, pp. 54–57.
- [4] D. Mandic and V. S. L. Goh, *Complex valued nonlinear adaptive filters: Noncircularity, widely linear and neural models*. John Wiley & Sons, 2009.
- [5] A. H. Sayed, *Fundamentals of adaptive filtering*. John Wiley & Sons, 2003.
- [6] S. Douglas, "Widely-linear recursive least-squares algorithm for adaptive beamforming," in *Proc. of the IEEE Intl. Conf. on Acoust. Speech and Signal Process. (ICASSP)*, April 2009, pp. 2041–2044.
- [7] P. Chevalier, J. P. Delmas, and A. Oukaci, "Properties, performance and practical interest of the widely linear MMSE beamformer for nonrectilinear signals," *Signal Processing*, vol. 97, pp. 269–281, 2014.
- [8] C. Jahanchahi, S. Kanna, and D. P. Mandic, "Complex dual channel estimation: Cost effective widely linear adaptive filtering," *Signal Processing*, vol. 104, pp. 33–42, 2014.
- [9] C. Hellings, M. Koller, and W. Utschick, "An impropriety test based on block-skew-circulant matrices," in *Proc. of the 19th International ITG Workshop on Smart Antennas*, March 2015, pp. 1–6.
- [10] A. Walden and P. Rubin-Delanchy, "On testing for impropriety of complex-valued Gaussian vectors," *IEEE Trans. Signal Process.*, vol. 57, no. 3, pp. 825–834, 2009.
- [11] P. Schreier, L. Scharf, and A. Hanssen, "A generalized likelihood ratio test for impropriety of complex signals," *IEEE Signal Process. Lett.*, vol. 13, no. 7, pp. 433–436, 2006.
- [12] J.-F. Cardoso and B. Laheld, "Equivariant adaptive source separation," *IEEE Trans. on Signal Process.*, vol. 44, no. 12, pp. 3017–3030, Dec 1996.
- [13] S. Kanna, S. Douglas, and D. Mandic, "A real time tracker of complex circularity," in *Proc. of the 8th IEEE Sensor Array and Multichannel Signal Process. Workshop (SAM)*, June 2014, pp. 129–132.
- [14] E. Ollila, "On the circularity of a complex random variable," *IEEE Signal Process. Lett.*, vol. 15, pp. 841–844, 2008.
- [15] P. Comon and C. Jutten, *Handbook of Blind Source Separation: Independent component analysis and applications*. Academic Press, 2010.
- [16] H. Li and T. Adali, "Algorithms for complex ML ICA and their stability analysis using Wirtinger calculus," *IEEE Trans. on Signal Process.*, vol. 58, no. 12, pp. 6156–6167, 2010.
- [17] J.-F. Cardoso and T. Adali, "The maximum likelihood approach to complex ICA," in *Proc. of the IEEE Intl. Conf. on Acoust. Speech and Signal Process. (ICASSP)*, May 2006, pp. 673–676.
- [18] S.-I. Amari and A. Cichocki, "Adaptive blind signal processing-neural network approaches," *Proc. of the IEEE*, vol. 86, no. 10, pp. 2026–2048, 1998.
- [19] A. Cichocki and S.-I. Amari, *Adaptive blind signal and image processing: Learning algorithms and applications*. John Wiley & Sons, 2002.